Ceramics International **22** (1996) 167–170

0272-8842(95)00075-5
0272-8842/96/$15.00

The Flexural Strength at High Temperature and Oxidation Behaviour of (Nb,Ti)C–Ni Composite

Ke-feng Cai, Ce-Wen Nan, Run-zhang Yuan & Xin-min Min

National Laboratory of Advanced Technology of Materials Compositing, Wuhan University of Technology, Wuhan, Hubei 430070, People's Republic of China

(Received 9 January 1995; accepted 22 March 1995)

Abstract: (Nb,Ti)C–Ni composite is prepared via hot isostatic pressing (HIP). Its flexural strength at elevated temperature is tested by means of three-point bending. The flexural strength, as a function of temperature, decreases at 700°C, and more rapidly decreases with further increase in temperature. At 1000°C, the flexural strength (about 325 MPa) is only 20% of that at room temperature. The oxidation behaviour of the composite in the temperature range from 850°C to 1100°C is also studied. The composite is oxidized into TiO_2, NiO and $NiTiO_3$ at high temperature. The oxidation kinetics are parabolic, with an activation energy of 234 kJ/mol.

1 INTRODUCTION

TiC has attracted considerable attention, because of its high melting point and high hardness. Various TiC-based cements, such as TiC–Ni, TiC–Mo_2C–Ni[1] and TiC–Mo–Nb–C[2] have been studied. However, as a high-temperature structural material, the major drawback with TiC is its brittleness, which is mainly attributed to covalent bonding. TiC consists mainly of covalent bonds and a few metal bonds. If the metal bond content can be increased, it is possible to modify the brittleness of TiC. Bogomolov[3] studied molybdenum-doped TiC ceramic and observed that the dopant molybdenum provides some improvement in brittleness of TiC. We have doped Nb into $TiC_{0.78}$ by means of arc melting, and investigated (Nb,Ti)C–Ni composite. The compatibility test[4] shows that the compatibility of (Nb,Ti)C with Ni is better than that of $TiC_{0.78}$ with Ni, and that the composite exhibits higher toughness than $TiC_{0.78}$–Ni.[5]

In this paper, the flexural strength at high temperature and oxidation behaviour of the composite are described.

2 EXPERIMENTAL PROCEDURE

Nonstoichiometric $TiC_{0.78}$ powder with an average particle size of 3 μm was used. (Nb,Ti)C powder (about 3 μm) was prepared by doping Nb into $TiC_{0.78}$ ($TiC_{0.78}$: Nb = 90 : 10 wt%) by means of arc melting. The (Nb,Ti)C powder and 35 wt% Ni powder were homogenized in alcohol for 10 h, and then dried under vacuum. Green bodies were produced by cold isostatic pressing (at 300 MPa). Specimens were fabricated by sintering under vacuum (about 133·3 Pa) at a temperature of 1350°C for 60 min, and then hot isostatic pressing (HIP) in argon at T = 1340°C and P = 182 MPa for 45 min. The resulting cylinders were cut into bars of 34 mm × 3 mm × 4 mm for measuring flexural strength at high temperature. The flexural strength of specimens at high temperature was tested by three-point bending over 30 mm span, with a crosshead speed of 0·5 mm/min. In the test, the specimens were held at the chosen temperature for 30 min before loading to ensure thermal equilibrium. The fracture surfaces were observed by means of scanning electron microscopy (SEM).

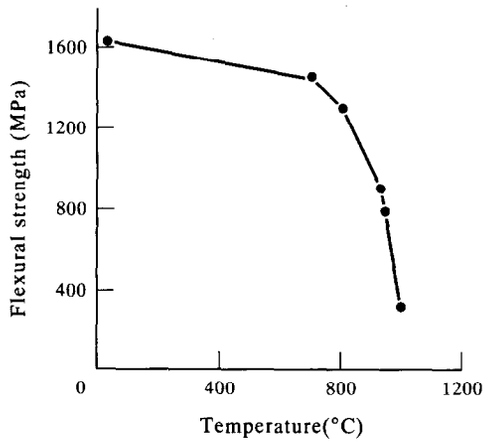

Fig. 1. Flexural strength as a function of temperature for (Nb,Ti)C–Ni composite.

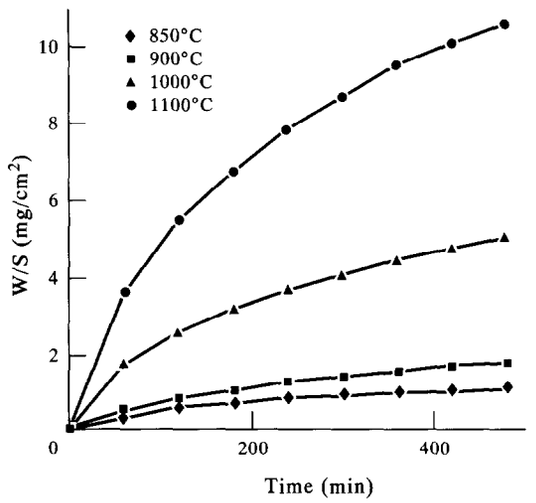

Fig. 3. Isothermal weight gain versus time for (Nb,Ti)C–Ni composite.

Short-term oxidation tests were conducted in static air. Oxidation temperatures ranged from 850°C to 1100°C, and the heating rate was 30°C/min. Samples were cleaned in acetone and weighed before and after oxidation with an electric-light microbalance capable of 1×10^{-5}g resolution. The surfaces of the oxidation scale were analyzed by X-ray diffraction and scanning electron microscopy.

3 RESULTS AND DISCUSSION

3.1 Flexural strength at high temperature

The flexural strength of the sample slowly decreases with increasing temperature between room temperature and 700°C and clearly decreases from 700°C (Fig. 1). The higher the temperature, the more rapidly the flexural strength decreases, and the flexural strength at 1000°C is only 20% of that at room temperature. The strength decrease at 700°C is due mainly to the relaxation of residual stresses introduced by machining;[6] this is also accompanied by the oxidation of the composite, introducing in this way new surface defects. On the other hand, the backscattered electron (BSE) image[5] showed that the composite consists of a network structure with (Nb,Ti)C particles as skeleton and Ni as binder phase. Because the melting point of Ni is 1433°C, when the sample is exposed at high temperature (around 1000°C) and stressed, the binder phase appears to be in a sticky state, which will weaken binding force between the binder phase and (Nb,Ti)C particles and then cause viscous flow of (Nb,Ti)C particles. These phenomena have been confirmed by the SEM photograph of the surface (Fig. 2). Figures 2(a) and (b) are fracture surface morphologies of the composite fractured at room temperature and at 1000°C, respectively. As seen from Fig. 2(a), the edges and corners of the particles are very sharp and there are many 'river'-like patterns in the fracture surface. In Fig. 2(b), the image of the fracture surface is dimmer, edges and corners are rounded, and there are some tough holes on the fracture surface, which cause the relaxation of the stresses. In particular, the viscous flow will make microcracks nucleate and grow, so the flexural strength of the sample sharply decreases.

3.2 Oxidation resistance

Figure 3 shows isothermal weight gain versus time for (Nb,Ti)C–Ni composite at various temperatures.

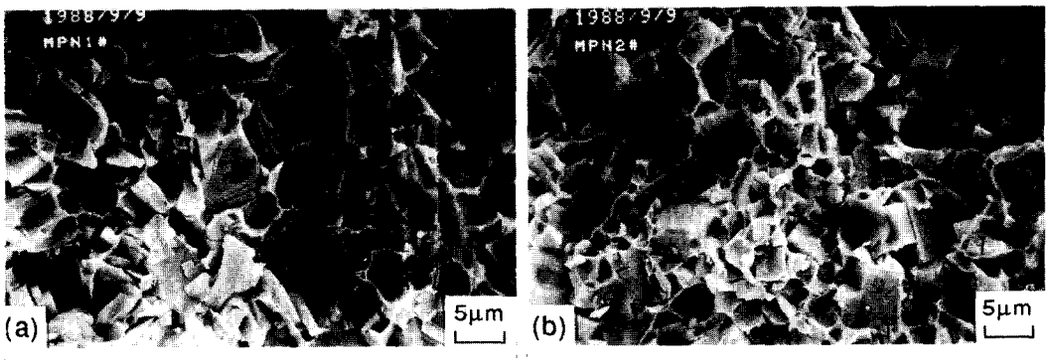

Fig. 2. SEM micrographs of fracture surface of (Nb,Ti)C–Ni composite fractured at (a) room temperature and (b) 1000°C.

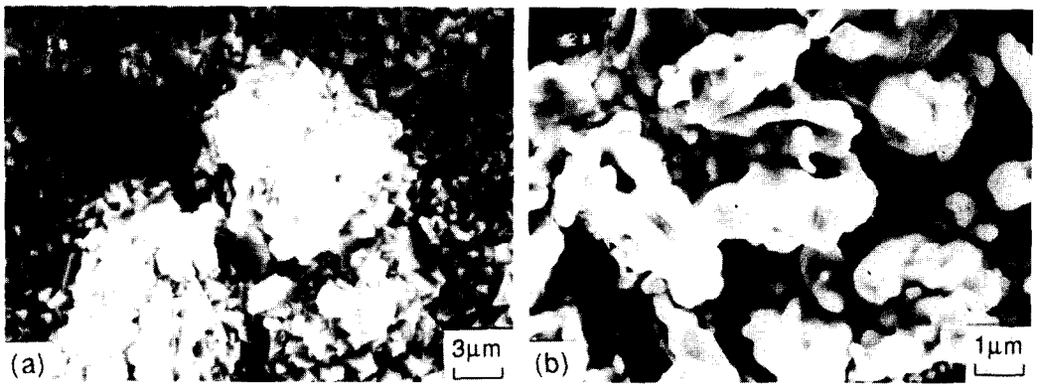

Fig. 4. SEM photographs of the composite oxidized for 8 h at (a) 850°C and (b) 1100°C.

It can be seen from Fig. 3 that the isothermal weight gain increases rapidly as the oxidation temperature increases.

3.2.1 Structure and morphology of the oxidized surface

The crystaslline phases detected on the oxidized surface were TiO_2, NiO and $NiTiO_3$ whose contents increased with increasing temperature. The formation of TiO_2, NiO and $NiTiO_3$ is supposed to occur in the following scheme:

$$TiC+O_2 = TiO_2+C \quad (1)$$

$$2C+O_2 = 2CO,\ 2CO+O_2=2CO_2 \quad (2)$$

$$2Ni+O_2 = 2NiO \quad (3)$$

$$TiO_2+NiO = NiTiO_3 \quad (4)$$

For simplicity, TiC in reaction (1) is used to represent (Nb,Ti)C since the content of Nb in $TiC_{0.78}$ is small. In fact, in the XRD pattern of the oxidized composite, the location of the peaks for TiO_2 was slightly deviated from their normal positions, which results from doping of Nb.

Figures 4(a) and (b) are the surface morphologies of the composite after oxidizing at 850°C and 1100°C for 8 h, respectively. They reveal that only part of the surface area of the composite was oxidized at 850°C, but a continuous oxide scale is formed at 1100°C.

Figure 5 is a section surface morphology of oxidized composite. It consists of three layers. The outer layer is a fully oxidized layer, the second layer is a transitional layer which is partly oxidized and porous, and the inner layer is a nonoxidized composite layer. There are cracks between the outer layer and the transitional layer and also between the transitional layer and the inner layer, which result from density difference between constituents. It is supposed that (Nb,Ti)C and Ni are oxidized according to reactions (1) and (3). An oxide film firstly forms at the surface of the sample, and then oxygen diffuses toward the reaction interface across the oxide film. At the same time titanium and nickel diffuse outward, so a porous Ti-depleted and Ni-depleted layer beneath the oxide film was formed.

3.2.2 Oxidation kinetics and mechanism

As seen from Fig. 3, the relation of the weight gain versus time followed a classical parabolic reaction equation

with
$$(W/S)^2 = Kt \quad (5)$$

$$K = K_0\exp(-E_a/RT) \quad (6)$$

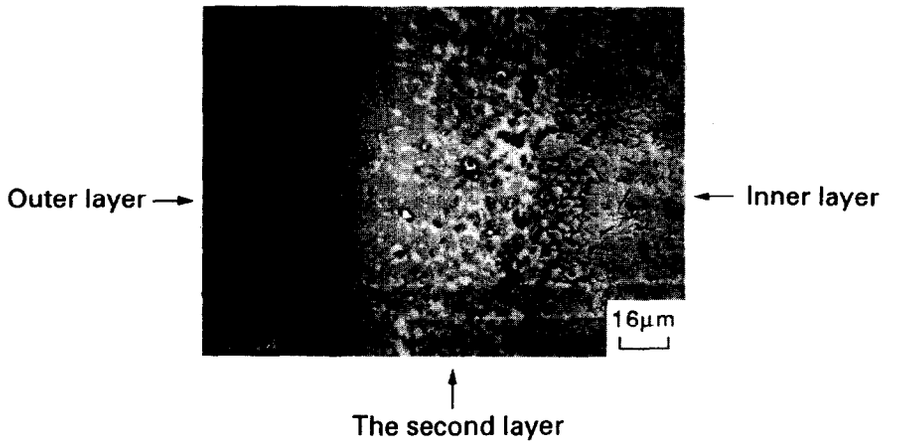

Fig. 5. Section face morphology of the (Nb,Ti)C–Ni composite oxidized at 1100°C for 8 h.

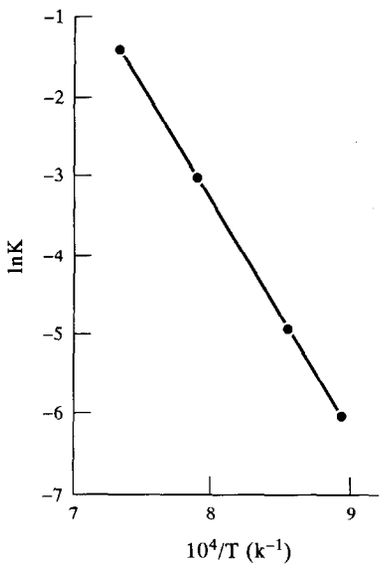

Fig. 6. Arrhenius plot of the oxidation rate constant, derived from a parabolic equation, for (Nb,Ti)C–Ni composite.

where W denotes the weight gain at time t, S is the geometrical area exposed to oxidation, K is the parabolic rate constant, E_a is the activation energy, and RT has its usual meaning. The parabolic kinetics indicate a diffusion mechanism as the rate-governing step. It can be known from the work of Suzuki *et al.*[7] that the product C of reaction (1) dissolves into TiO_2 at first and then desorbs, in the form of CO or CO_2, toward atmosphere across the oxide layer. So, across the oxide scale formed by a layer of TiO_2, NiO and $NiTiO_3$ crystals, the diffusion of O_2 from the atmosphere to the reaction interface or the desorption of CO and CO_2 from the reaction interface to the atmosphere is proposed as the primary diffusion mechanism controlling oxidation. Figure 6 shows an Arrhenius plot for the oxidation reaction-rate constant, K, obtained from the parabolic kinetics (850–1100°C). For this composite the apparent value of E_a is about 234 kJ/mol.

4 CONCLUSIONS

(1) In an oxidative atmosphere, the composite is oxidized into TiO_2, NiO, and $NiTiO_3$ at high temperature. The flexural strength decreases with increasing temperature.

(2) In the range between 850°C and 1100°C, the classic parabolic kinetics reveal a diffusion mechanism due to the diffusion of O_2 or the desorption of CO and CO_2 through the oxide scale.

REFERENCES

1. HUMENIK, M. J. & PARIKH, N. M., *J. Am. Ceram. Soc.*, **39** (1956) 60.
2. KOMACK, M. & LANGE, D., *Int. J. Powder Metall. & Powder Techn.*, **18**(4) (1982) 314.
3. BOGOMOLOV, A. M., *Russian Poroshk. Metall. (Kiev)*, **3** (1988) 61.
4. CAI, K. F., DING, W. C. & YUAN, R. Z., In *Proc. Symp. 7th National Conference on Composite Materials*, Dalian, China, H-47-1, 1992.
5. CAI, K. F., YUAN, R. Z., PI, Z. J. & DING, W. C., In *Proc. Symp. 1st Pacific Rim International Conference on Advanced Materials and Processing*. TMS, Warrendale, 1993, p. 909.
6. JOHNSON-WALLS, D., EVANS, A. G., MARHALL, D. B. & JAMES, M. R., *J. Am. Ceram. Soc.*, **69** (1986) 44.
7. SUZUKI, H., MATSUBARA, H. & KAYASHI, K., *J. Japan Inst. Metals*, **46**(6) (1982) 651.